ACS Catalysis

Research Article

pubs.acs.org/acscatalysis

Influence of the Carbon−Carbon Bond Order and Silver Loading on the Formation of Surface Species and Gas Phase Oxidation Products in Absence and Presence of NO_x over Silver-Alumina Catalysts

Hanna Härelind,* Fredrik Gunnarsson, Seyyed Majid Sharif Vaghefi, Magnus Skoglundh, and Per-Anders Carlsson

Competence Centre for Catalysis, Department of Chemical and Biological Engineering, Chalmers University of Technology, SE-412 96 Göteborg, Sweden

ABSTRACT: The influence of carbon−carbon bond order, here systematically represented by prototypical C_2H_6, C_2H_4, and C_2H_2, on the formation of oxidation products and surface species in the absence and presence of NO has been studied for silver-alumina catalysts with different silver loadings (2 and 6 wt %). The catalysts were prepared with a sol−gel method including freeze-drying, which results in small silver species uniformly distributed throughout the alumina matrix. The performance of the catalysts was investigated by temperature programmed extinction-ignition experiments using a continuous gas flow reactor. The evolution of surface species during reactant step-response experiments was studied in situ by diffuse reflection Fourier transform infrared spectroscopy. The results show that activation for oxidation generally proceeds more easily with increasing bond order of the hydrocarbon. For example, C_2H_2 shows the highest conversion at low temperatures. Furthermore, the use of hydrocarbons with high bond order, that is, C_2H_2, as reductant for lean NO_x reduction results not only in the highest peak activity but also in considerable high activity in a wide temperature range mainly thanks to high activity at low temperature. With increasing silver loading, the oxidation reactions are favored such that both the hydrocarbon and the NO activation occur at lower temperatures. Several types of adsorbates, for example, carbonate, acetate, formate, enolic and isocyanate/cyanide surface species, are present on the catalyst during reaction. Generally the nature of the surface species and likely also the surface processes are more influenced by the carbon−carbon bond order than the silver loading. This needs to be considered when designing catalysts for emission control systems. Especially for applications using homogeneous fuels with short hydrocarbons, this may provide opportunities to tailor the catalyst functionality for the needs at hand.

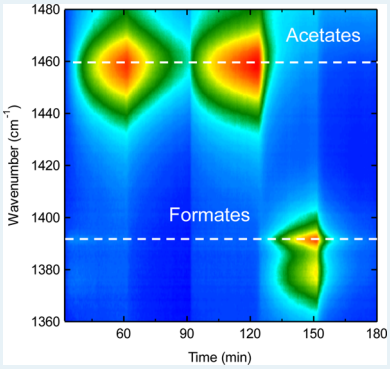

KEYWORDS: *hydrocarbon oxidation, lean NO_x reduction, silver-alumina, ethane, ethene, ethyne, transient experiments, in situ DRIFTS*

1. INTRODUCTION

Silver-alumina is a well-known catalyst for epoxidation of ethene to ethene oxide, see, for example, ref 1 and references therein. During the past couple of decades this system has been studied for selective catalytic reduction of NO_x with hydrocarbons and oxygenates (HC-SCR)[2−11] and more recently also with ammonia (NH_3-SCR), for example, ref 12, as reducing agent. The functionality of both the silver and alumina sites is very different in these applications. For epoxidation large silver particles on a low surface area alumina is required,[13] while in the case of lean NO_x reduction a highly dispersed silver phase on a high surface area alumina is beneficial or even needed.[14−16]

For HC-SCR the Ag/Al_2O_3 system has been studied extensively. It has for instance been shown that very small silver clusters ($Ag_{n<8}$) to a greater extent provide active sites for lean NO_x reduction with hydrocarbons as compared to larger silver crystallites.[17] Despite the numerous studies, the structure and chemical state of silver in such clusters remain elusive. For example metallic silver, silver oxides, and silver aluminate have all been suggested as the main active phase.[17,18] It has been shown, however, that different forms of oxidized silver species, like Ag^+, Ag_2O, or silver aluminate, favor the reduction of NO to N_2[19−22] whereas metallic silver particles are more active for oxidation reactions.[23−25] Further, it has been suggested that $Ag_n^{\delta+}$ clusters are highly active for the HC-SCR process,[26] particularly for the activation of the reducing agent by partial oxidation.[11] These findings indicate that catalysts, that are active for NO_x reduction by hydrocarbons most likely contain highly dispersed ionic, oxidized and/or $Ag_n^{\delta+}$ silver species.

Recently Kannisto et al.[15] showed that preparation of silver-alumina catalysts by a sol−gel method results in a higher proportion of nonmetallic silver, that is, clusters and/or oxidized silver species, as compared to samples prepared by

Received: March 16, 2012
Revised: May 31, 2012
Published: June 8, 2012

   dx.doi.org/10.1021/cs3001754 | ACS Catal. 2012, 2, 1615−1623

conventional impregnation. Furthermore, by using freeze-drying instead of thermal drying of the formed gel, a higher dispersion of the silver can be achieved.[15] The authors also show that significant differences in catalytic properties can be obtained by varying the silver content. More silver results in catalysts that likely contains a higher amount of oxidizing sites, at least when using propene and *n*-octane as reducing agent.[15]

In the present study the oxidative function of the silver-alumina system in the absence and presence of NO is specifically addressed. In particular the influence of the carbon−carbon bond order, here systematically represented by prototypical C_2H_6, C_2H_4 and C_2H_2, on the formation of surface species and gas phase products is considered for silver-alumina catalysts with different silver loading.

2. EXPERIMENTAL SECTION

2.1. Catalyst Preparation and Characterization. Two silver-alumina catalysts (2 and 6 wt % Ag) were prepared using a single step sol−gel method including freeze-drying of the formed gel, as described by Kannisto et al.[15] Briefly, aluminum isopropoxide (AIP) was added to milli-Q water and heated to 82 °C, subsequently silver nitrate ($AgNO_3$) solution was added under continuous stirring (Table 1). The pH was adjusted to 4.5 using HNO_3 (10%) and a sol was formed. The sol was stirred for 12 h, and a major part of the solvent was then removed under reduced pressure at 35 °C to form a gel. Finally the sol−gel was freeze-dried and calcined in air (6 h, 600 °C).

Table 1. Nominal Silver Content and Amount of Precursor Used in the Sample Preparation

sample	nominal Ag content (wt %)	AIP (g)	$AgNO_3$ (g)
2 wt % Ag−Al_2O_3	2	19.63	0.16
6 wt % Ag−Al_2O_3	6	18.85	0.47

Following the procedure outlined in ref 15, the as prepared powder samples were coated onto monolith substrates (L = 20 mm, ⌀ = 25 mm), which were cut from a commercial cordierite honeycomb structure (Corning, 400 cpsi). Briefly, the silver-alumina powder was mixed with boehmite (Disperal Sol P2; Condea) in a weight ratio of 4:1 and then water (milli-Q) was added under vigorous stirring, forming a slurry with a dry content of 20 wt %. The monolith was coated by immersion in the slurry. Excess slurry was removed by gently blowing air through the channels. The coated monolith was then dried at 90 °C for 15 min and subsequently calcined (500 °C, 5 min). The procedure was repeated until catalytic material corresponding to 20% of the total weight was deposited on the monolith. The monolith was finally calcined in air for 3 h at 600 °C.

The specific surface area and the pore-size distribution of the powder samples were determined by N_2 sorption at 77 K using a Micromeritics TriStar instrument, according to the Brunauer−Emmett−Teller (BET)[27] and Barrett−Joyner−Halenda (BJH)[28] method, respectively. The samples were dried at 200 °C in vacuum for 2 h before analysis. The results are summarized in Table 2.

2.2. Flow Reactor Experiments. The catalytic activity for oxidation of hydrocarbons in absence and presence of NO_x over the samples was studied in a flow reactor system described in detail elsewhere.[29,30] Briefly, the reactor consists of a horizontal quartz tube heated by a heating coil, where the temperature is measured by two thermocouples (type K), placed 15 mm before the sample and inside at the rear end of the monolith sample, respectively. The inlet gas composition is controlled by separate mass flow controllers (Bronkhorst Hi-Tech, lowΔP) and the outlet gas composition is measured by an FTIR analyzer (MKS MultiGas 2030 HS).

The samples were pretreated with 10% O_2 (550 °C, 30 min) and then temperature programmed experiments (550 → 50 → 550 °C, 5 °C/min) with 10% O_2 and 600 ppm of either C_2H_6, C_2H_4 or C_2H_2 were performed. Subsequently, 200 ppm NO was added to the feed gas and the ramp experiments were repeated. During all experiments the total gas flow was kept constant at 3500 mL/min, corresponding to a space velocity (GHSV) of 32000 h^{-1}.

2.3. In situ DRIFT Spectroscopy. In situ Fourier transform infrared spectroscopy measurements were performed in diffuse reflectance mode (DRIFT) using a Bio-Rad FTS6000 spectrometer equipped with a high temperature reaction cell (Harrick Scientific, Praying Mantis).[31,32] Gases were introduced to the DRIFT cell via separate mass flow controllers (Bronkhorst Hi-Tech, low ΔP), and the gas composition after the cell was probed using a quartz capillary and continuously measured by a quadrupole mass spectrometer (Balzers QMS 200).

The sample was pretreated with 10% oxygen at 500 °C for 30 min and then pure Ar at 450 °C for 20 min at a total flow rate of 100 mL/min. Background spectra (60 scans at a resolution of 1 cm^{-1}) were collected for fresh samples under Ar atmosphere. Step-response experiments were subsequently performed at 450 °C, where the hydrocarbon (C_2H_4 and C_2H_2) and NO supply was switched on and off, according to Table 3. IR spectra with 1 cm^{-1} spectral resolution were collected with an acquisition frequency of 0.1 Hz.

Table 3. Gas Composition during the Different Steps in the Step-Response Experiment Sequence

step	C_2H_4 or C_2H_2 (ppm)	NO (ppm)	O_2 (vol %)
1	600	0	10
2	0	0	10
3	600	0	10
4	600	600	10
5	0	600	10

3. RESULTS AND DISCUSSION

3.1. Oxidation Products and NO_x Reduction. The catalytic activity and selectivity for oxidation of hydrocarbons

Table 2. Specific Surface Area and Pore Size Distribution of the Prepared Samples

sample	specific surface area [m^2/g]	total pore volume [cm^3/g]	BJH absorption cumulative pore volume [cm^3/g]	absorption average pore width [Å]	BJH absorption average pore diameter [Å]	BJH desorption average pore diameter [Å]
2 wt % Ag−Al_2O_3	193	0.25	0.24	52	46	40
6 wt % Ag−Al_2O_3	184	0.22	0.21	47	42	37

dx.doi.org/10.1021/cs3001754 | ACS Catal. 2012, 2, 1615−1623

with different carbon−carbon bond order (i.e., alkane, alkene, and alkyne), both in the absence and presence of NO, over the two catalyst samples were evaluated in flow reactor experiments. The results are summarized in Figures 1 and 2. Figure 1

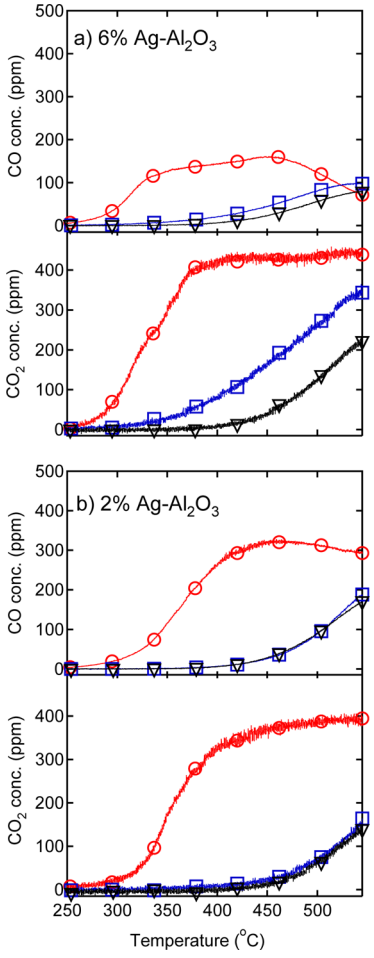

Figure 1. Formation of CO and CO_2 during temperature programmed extinction experiments with C_2H_2 (circle), C_2H_4 (square), and C_2H_6 (triangle) over Ag/Al_2O_3 catalyst with (a) 6 wt % and (b) 2 wt % nominal silver content. Inlet gas composition: 600 ppm C_2 hydrocarbon, 10% O_2, Ar balanced. GHSV: 32 000 h^{-1}.

shows the formation of CO and CO_2 when C_2 hydrocarbons are oxidized with O_2 over 2 and 6 wt % Ag−Al_2O_3 catalysts during extinction (cooling) ramp experiments. In general the hydrocarbon oxidation proceeds at lower temperatures and results in higher CO_2 formation over the 6 wt % Ag sample as compared to the 2 wt % Ag sample. This is particularly evident in the case of C_2H_4 oxidation, which starts around 350 °C over the 6 wt % Ag sample but not below 450 °C over the 2 wt % Ag sample. For both catalysts, the lowest activation temperature is observed for ethyne (C_2H_2) oxidation, which starts around 270 and 300 °C for the 6 and 2 wt % Ag samples, respectively. The formation of CO and CO_2 is also significantly higher during oxidation of C_2H_2 as compared to the other hydrocarbons. The highest temperature for oxidation onset is observed for C_2H_6, and the oxidation pattern is generally similar for both catalysts although the CO_2/CO ratio is slightly higher over the 6 wt % Ag sample. Over both catalysts, trace amounts of formaldehyde (detected less than 5 ppm) were observed for ethyne oxidation

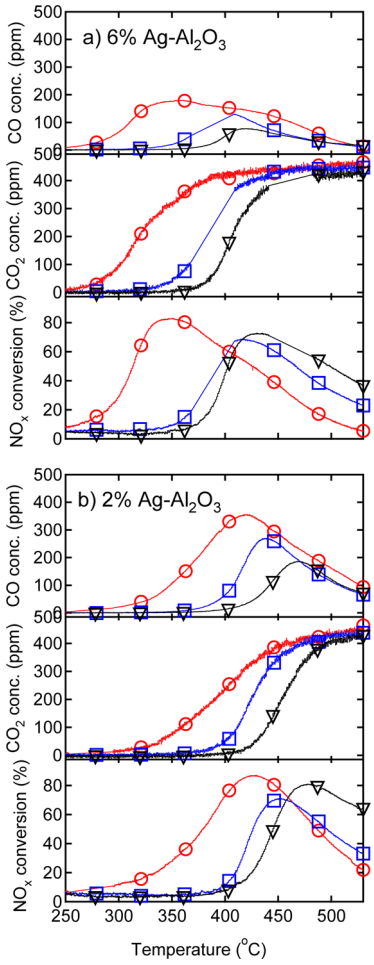

Figure 2. Formation of CO, CO_2 and reduction of NO_x during temperature programmed extinction experiments with C_2H_2 (circle), C_2H_4 (square), and C_2H_6 (triangle) over Ag/Al_2O_3 catalyst with (a) 6 wt % and (b) 2 wt % nominal silver content. Inlet gas composition: 200 ppm NO, 600 ppm C_2 hydrocarbon, 10% O_2, Ar balanced. GHSV: 32 000 h^{-1}.

and minor amounts of methane (less than 5 ppm) were detected for all hydrocarbons.

Figure 2 shows the NO_x reduction and CO and CO_2 formation during oxidation of C_2 hydrocarbons in the presence of NO and excess O_2 over the 2 and 6 wt % Ag−Al_2O_3 catalysts during extinction ramp experiments. The NO_x reduction pattern is in general similar for both catalysts although the temperature windows are shifted to lower temperatures and the maximum NO_x reduction is slightly lower for the 6 wt % Ag sample. The highest NO_x reduction is achieved when C_2H_2 is used as reducing agent, over both catalysts, reaching 87% at 427 °C for the 2 wt % Ag sample. For both catalysts the C_2H_2 also shows the widest temperature window for NO_x reduction. The maximum NO_x reduction for C_2H_4 and C_2H_6 is 71% and 81%, respectively, over the 2 wt % Ag sample and around 70% over the 6 wt % Ag sample. The temperature windows for NO_x reduction with these hydrocarbons are similar, showing no significant activity below 350 and 400 °C for the 6 and 2 wt % Ag samples, respectively.

The hydrocarbon oxidation profile in the presence of NO is similar for both catalysts, however, significantly different compared to oxidation in absence of NO. The activation temperature for oxidation of all hydrocarbons is lower over the

dx.doi.org/10.1021/cs3001754 | ACS Catal. 2012, 2, 1615−1623

6 wt % Ag sample, while the CO formation is higher for the 2 wt % Ag sample. Particularly different, as compared to oxidation without NO, is the activation of the C_2H_4 and C_2H_6 hydrocarbons, which starts at lower temperatures in the presence of NO, and the formation of both CO and CO_2 is significantly increased. The C_2H_2 hydrocarbon again shows the lowest activation temperature for oxidation and follows the same trend as without NO, that is, slightly lower activation temperature for the 6 wt % Ag sample. The differences between hydrocarbon oxidation in absence and presence of NO may be explained by the fact that formed NO_2 and nitrates are stronger oxidants than O_2[31,33] so that the oxidation of hydrocarbons can be promoted. When NO was present in the feed, trace concentrations (<5 ppm) of NH_3, N_2O, and HCHO were detected. An interesting feature is that the temperature corresponding to the maximum CO formation coincides with the temperature for maximum NO_x reduction, for both catalysts. This is likely related to the partial oxidation of the hydrocarbons, as CO is a product of partial oxidation. It is known that partially oxidized hydrocarbons are key intermediates in the SCR process, so the temperature corresponding to the maximum formation of partially oxidized hydrocarbons is likely close to the temperature for maximum NO_x reduction. Another possibility is that CO itself may act as an intermediate in the lean NO_x reduction and/or CO preferably reacts with NO_x compared to oxygen.

The flow reactor experiments show that increasing the silver loading, here from 2 to 6 wt %, results in a shift of the activation temperature for oxidation of the hydrocarbons, and a shift and a broadening of the NO_x reduction temperature window. This is probably connected to the presence of a higher amount of metallic silver species in the 6 wt % Ag catalyst compared to the 2 wt % Ag catalyst, facilitating total oxidation in agreement with previous studies.[15,21] This is further supported by the lower CO and higher CO_2 concentrations observed for the 6 wt % Ag catalyst, compared to the 2 wt % Ag catalyst. The activation of hydrocarbons at low temperature accompanied by high NO_x reduction ability over the catalysts indicate high distribution of both oxidizing (metallic silver, $Ag_n^{\delta+}$ clusters) and reducing (such as Ag^+, Ag_2O) silver species throughout the catalytic material. For the 2 wt % Ag-alumina sample UV−vis experiments show the presence of isolated silver ions (Ag^+) and small silver clusters ($Ag_n^{\delta+}$).[34] However, the presence of metallic silver is less certain.[34] Furthermore, the formation of $Ag_n^{\delta+}$ clusters during SCR conditions has been demonstrated by UV−vis and EXAFS, as reported by, for example, Breen et al.[35] For the small and relatively stable hydrocarbons used in this work rather strong oxidation sites are needed in addition to the NO reduction sites.

From the flow reactor results, the activation of C_2 hydrocarbons over the 2 and 6 wt % Ag catalysts can be arranged in the order: $C_2H_2 > C_2H_4 > C_2H_6$. However, the ability for these hydrocarbons to act as reducing agents for NO_x in excess oxygen follows a different order: $C_2H_2 > C_2H_6 > C_2H_4$. One can envisage that the C_2H_2, apparently being the most easily oxidized, also will be the most active as reducing agent for NO_x reduction. In parallel one would anticipate that C_2H_4 would be a more effective reducing agent for NO_x compared to C_2H_6. However, because of steric hindrance as discussed below, the interaction with the catalyst surface may not be the most important issue here. Instead this may be an effect of hydrogen, as C_2H_6 can provide a higher amount of hydrogen to the active surface, compared to C_2H_4, and the silver-alumina system is known to benefit from hydrogen addition.[36]

The C−C bond strength for ethane, ethene, and ethyne is 376, 727, and 965 kJ/mol, respectively, according to Blanksby and Ellison.[37] It may seem unexpected that ethyne is more easily oxidized than ethene and ethane, as the former hydrocarbon has the strongest C−C bond, that is, a triple bond. However, to oxidize ethyne (and ethene) the rate determining step is likely not to totally break the C−C bond but instead to activate the molecule. This can be compared to the epoxidation reaction forming ethene oxide from ethene.[38] The electrons in the π-bonds in ethene and especially ethyne, for which the π-electron cloud has a cylindrical shape, can easily interact with the catalyst surface and thereby form new bonds between the unsaturated hydrocarbon and the surface. These surface species are susceptible toward further reactions, for example addition reactions with oxygen to form surface oxygenates, which are essential in NO_x reduction.[18] However, a too high amount of available surface oxygen would lead to oxidative cleavage of the hydrocarbon, facilitating formation of CO and eventually complete combustion. Contrarily for ethane to form the same type of surface oxygenates, hydrogen abstraction is necessary. Thus activation of the C−H bond is important for ethane oxidation.

The difference in oxidation between the C_2 hydrocarbons can also be discussed in terms of steric hindrance. The ethyne molecule, being straight, can easily reach a favorable position on the surface. In the case of ethene and ethane this position is more difficult to reach because of steric hindrance, where the ethene molecule can interact effectively only in one direction (i.e., in the plane parallel to the surface) and the ethane molecule has methyl end-groups resulting in a weaker interaction with the catalyst surface. A parallel may be drawn to previous work on oxidation of propene and propane[39,40] and NO_x reduction with either propene or propane[41] over Pt-based catalysts. These studies showed that propene can easily be oxidized over the Pt surface, cleaning the surface from oxygen, while in the case of propane the Pt surface will instead be oxygen poisoned, since propane interacts less effectively with the Pt surface. Steric effects have also been discussed for C−H bond interaction with the catalyst surface. For instance Siegbahn[42] investigated the relation between hydrocarbon activation and C−H bond strength for ethyne, ethene, and methane and found that for second row transition metals acting as catalyst this relation is inverse. Even though ethyne possesses the strongest C−H bond[42,43] among these hydrocarbons, the activation barrier for breakage of this bond is the lowest. This is explained by a steric effect, where C−H activation needs the metal, second row transition metal in this case, to interact more efficiently in a side way orientation with the C−H bond, which is facilitated for the straight ethyne molecule.[42] However, in the present case the C−C bond activation is likely more important than the activation of the C−H bond.

Furthermore, the difference in steric hindrance is largely reflected in the sticking probability. As comparative studies on the sticking probabilities of C_2 hydrocarbons on silver are rare, we here attempt to discuss this matter generally, based on observations for other systems. It has, for instance, been shown that the sticking probability for C_2 (C_2H_x, $x = 0-6$) hydrocarbons on diamond (111) generally decreases as the number of hydrogen atoms in the molecule increases.[44] This is caused by an increased reflection of the approaching molecule by shielding because of the higher number of hydrogen

dx.doi.org/10.1021/cs3001754 | ACS Catal. 2012, 2, 1615−1623

Table 4. Summary of Observed Peaks with Relevant Literature References

surface species	wavenumber (cm^{-1})	system	ref.
CHO species			
bidentate carbonate	1620−1530, 1270−1250	Me/oxide	46
	1680−1530, 1440−1320	Me/oxide	47
monodentate carbonate	1530−1470, 1370−1300	Me/oxide	46
	1550−1480, 1410−1340	Me/oxide	47
formate	1590, 1390, 1378	Al_2O_3	51
	3005, 2910, 1595, 1390, 1380, 1375	Al_2O_3, Ag/Al_2O_3	23,55
	1390, 1376	Al_2O_3	52
	1392, 1377	Ag/Al_2O_3	21,48
acetate	1580−1570, 1465−1460	Ag/Al_2O_3	50−52
	1570, 1466, 1394	Ag/Al_2O_3	53
	1590−1550, 1465, 1355	Al_2O_3	52
acetate or free carboxylate species	1576, 1458	Ag/Al_2O_3	21,48,49
acrylate species	1645, 1570, 1455, 1392−1378, 1297	Ag/Al_2O_3	48,54
(ethyl) carbonate	1630, 1412, 1340	Ag/Al_2O_3	55
	1626, 1412, 1336	Ag/Al_2O_3	50
enolic species	1633, 1416, 1336	Ag/Al_2O_3	56
	1630, 1412, 1333	Ag/Al_2O_3	53
NOx species			
monodentate nitrate	1530−1480, 1290−1250	Me/oxide	57
	1560, 1558, 1556, 1550, 1297, 1250, 1245	Ag/Al_2O_3	7,16,56
bidentate nitrate	1565−1500, 1300−1260	Me/oxide	57
	1590, 1586, 1585, 1304, 1298, 1295, 1248	Ag/Al_2O_3	7,16,56
bridging nitrate	1650−1600, 1225−1170	Me/oxide	57
	1615, 1614	Ag/Al_2O_3	7,16,56
nitrosonium ion (NO^+)	2311−2237	Ag/Al_2O_3	54
-NCO/-CN species			
-NCO	2255 (Al(VI)-NCO), 2228 (Al(IV)-NCO)	Ag/Al_2O_3	55
	2232 (Ag^+-NCO)	Ag/Al_2O_3	21
	2230	Al_2O_3, Ag/Al_2O_3	23
	2229	Ag/Al_2O_3	53
-CN	2155, 2127	Ag/Al_2O_3	55
	2162, 2130	Ag/Al_2O_3	21
	2135	Al_2O_3, Ag/Al_2O_3	23

atoms.[44] A comparison of C_2H_2 and C_2H_4 adsorption on Rh(100) shows that the sticking probability for ethyne remains almost constant up to a coverage of approximately 0.3 ML, while for C_2H_4 the sticking probability significantly decreases with increasing coverage.[45] This implies that incoming ethyne molecules more easily achieve sufficient space on the surface to decompose to C═CH, as compared to ethene.[45] In conclusion, the hydrocarbon activation is highly dependent on C−C bond strength, steric effects, and sticking probability.

3.2. Surface Species and Reaction Mechanisms.

3.2.1. Surface Species. In situ DRIFT spectroscopy measurements were performed to follow the evolution of surface species, in particular hydrocarbon derived species during oxidation of C_2H_2 and C_2H_4 in presence and absence of NO. In Table 4 the assignments of IR absorption bands are summarized. Figure 3 shows the evolution of surface species in the step-response experiments over the 2 and 6 wt % Ag samples at 450 °C, with ethene as reductant. When ethene and oxygen are introduced to the 6 wt % Ag catalyst (step 1), bands at 1248, 1296, 1459, 1545, 1570, 1588, 2906, and 2997 cm^{-1} appear. The bands at 1245, 1296, and 1545 cm^{-1} are assigned to monodentate and/or bidentate carbonates,[46,47] and the bands at 1459 and 1570 cm^{-1} are attributed to acetate and/or free carboxylate species.[21,48−53] Alternatively, the bands at 1296, 1459, 1570 cm^{-1} may be assigned to acrylate species.[48,54] The peak at 1588 cm^{-1} and the weak bands at 2906 and 2997 cm^{-1} (not shown) can be ascribed to formate species.[23,55] For the 2 wt % Ag catalyst, bands at 1250, 1294, 1378, 1391, 1457, 1545, 1588 cm^{-1} and weak peaks at 2906 and 2997 cm^{-1} were observed. A majority of these bands are similar to the ones observed for the 6 wt % Ag catalyst and are assigned accordingly. Interestingly, the bands at 1378 and 1391 cm^{-1} are only observed for the 2 wt % Ag sample and may be assigned to formate species[21,23,48,52,55] and/or to acrylate species.[48,54]

In step 2, when the ethene supply was switched off, the acetate bands at 1459 and 1570 cm^{-1} gradually decrease for both catalysts. After ethene was switched on again (step 3), the acetate bands grow and reach similar absorption as in step 1. After adding NO (step 4) new bands at 1245, 1292, 1378, 1391, 2245 cm^{-1} appear similarly for both catalysts, while the acetate band at 1459 cm^{-1} disappears. The other band of acetate at 1570 cm^{-1} was not distinguishable, likely because of overlapping bands. Bands in the region 1600−1200 cm^{-1} are attributed to both carbonate/carboxylate species and to nitrite/nitrate species (Table 4), which results in several overlaps and hence unique assignments are not straightforward. The peaks at 1245 and 1292 cm^{-1} are attributed to monodentate and/or bidentate nitrates,[7,16,56,57] and the weak band at 2245 cm^{-1} (not shown) is assigned to isocyanate species (-NCO)[55] and/or

dx.doi.org/10.1021/cs3001754 | ACS Catal. 2012, 2, 1615−1623

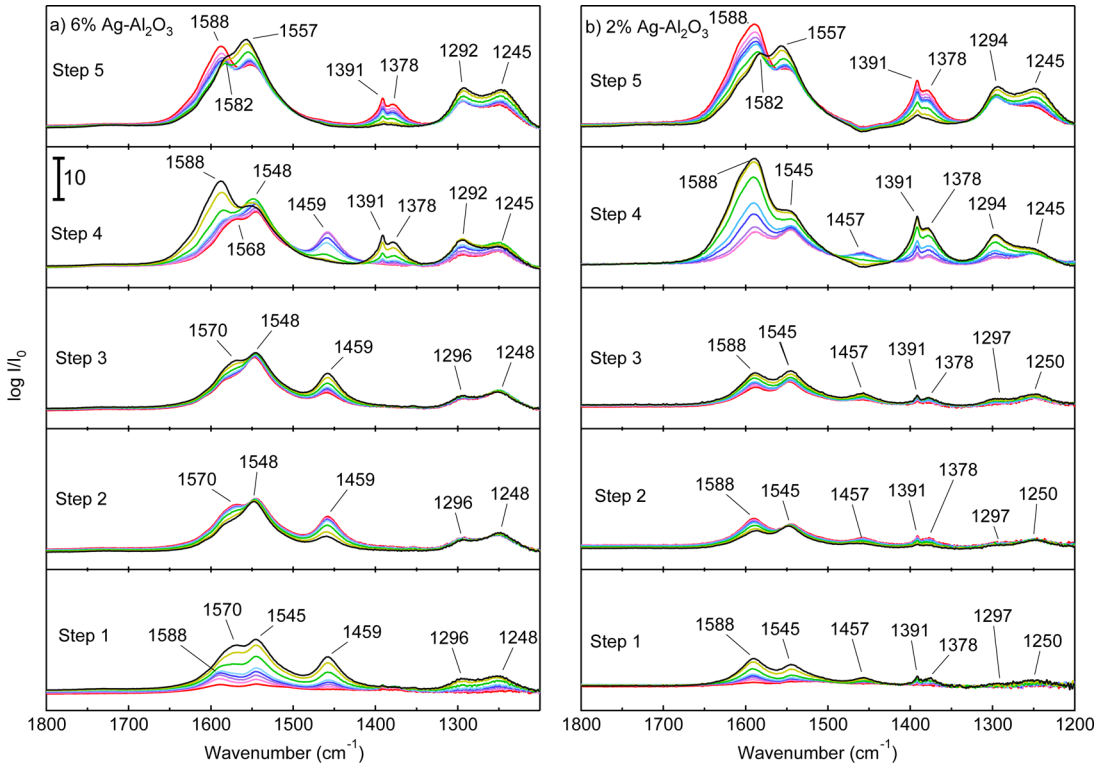

Figure 3. Evolution of surface species during step response experiments with C_2H_4 recorded in DRIFTS at 450 °C over Ag/Al_2O_3 catalyst with (a) 6 wt % and (b) 2 wt % nominal silver content, after 1 min (red), 2 min (pink), 3 min (purpule), 4 min (blue), 5 min (light blue), 10 min (green), 20 min (light green), and 30 min (black) gas exposure. Inlet gas composition: step 1: $C_2H_4 + O_2$; step 2: O_2; step 3: $C_2H_4 + O_2$; step 4: $C_2H_4 + NO + O_2$; step 5: $NO + O_2$. Contents: 600 ppm NO, 600 ppm C_2H_4, 10% O_2, Ar balanced.

nitrosonium ions (NO^+).[54] The intensity of the formate bands at 1588, 2906, and 2997 cm^{-1} seems to increase for both catalysts during this step, while the intensity of the carbonate bands is rather reduced. Upon switching off the ethene supply (step 5) new bands at 1557 and 1582 cm^{-1} are observed for both catalysts, corresponding to monodentate and/or bidentate nitrate species.[7,16,56,57] The formate bands gradually decrease, and the intensity of the nitrate bands around 1250 and 1290 cm^{-1} increases simultaneously.

Figure 4 shows the evolution of surface species during step-response experiments with C_2H_2 over the 2 and 6 wt % Ag catalysts. After introducing ethyne and oxygen to the 2 wt % Ag sample in the first step (Figure 4b), several bands that have previously been assigned to carbonate, acetate, acrylate, and formate species (Table 4) appear at 1298, 1391, 1460, 1539, 1576 cm^{-1}. Furthermore, a new band appears at 1354 cm^{-1}, which likely can be ascribed to acetate species.[52] For the 6 wt % Ag catalyst, bands at 1298, 1340, 1412, 1460, 1542, 1576, and 1627 cm^{-1} are observed. Some of these bands are assigned previously, and the bands at 1340, 1412, and 1627 cm^{-1} are assigned to enolic and/or ethyl carbonate species.[47,50,53,55,56] In addition, some minor peaks in the 3000−2900 cm^{-1} region are observed for both catalysts (not shown), which previously have been assigned to formate species.[23,55]

Switching off the ethyne supply (step 2) results in reduced intensity for all bands except for the band at 1248 cm^{-1}, possibly owing to formation of carbonate species in the presence of oxygen.[46] The intensity of the bands in this step is more reduced for the 6 wt % Ag catalyst compared to the 2 wt % Ag catalyst, which likely is due to the presence of more metallic silver particles in the 6 wt % Ag catalyst, facilitating the oxidation of surface species. When introducing ethyne in step 3, all peaks reappear except for the peak at 1248 cm^{-1}, which diminishes. However, the intensity of these bands over the 6 wt % Ag catalyst is lower compared to step 1. When NO is added to the feed gas containing ethyne and oxygen (step 4) new peaks arise at 2124 and 2228 cm^{-1} and at 2124, 2151, and 2228 cm^{-1} for the 6 and 2 wt % Ag catalyst, respectively (Figure 5). The peaks at 2124 and 2151 cm^{-1} are ascribed to cyanide (-CN) species bound to Ag or Al sites,[21,23,55] and the peak at 2228 cm^{-1} is attributed to isocyanate (-NCO) species attached to Ag or Al sites on the catalyst surface.[21,23,53,55] In step 5, after removing ethyne from the feed gas, bands at 1248, 1298, 1558, and 1580 cm^{-1} appear, which previously have been assigned to monodentate and/or bidentate nitrates. During this step the intensity of the other bands resulting from the ethyne reaction (carboxylates and carbonates) decreases. In addition, a shoulder at 2250 cm^{-1} appears on the peak at 2228 cm^{-1}, after a few minutes on stream in step 5, this shoulder likely reflects -NCO species bound to Al-sites.[55]

3.2.2. Mechanistic Interpretations. The initial steps in the HC-SCR mechanism are considered to be formation of surface nitrates by oxidation of adsorbed NO_x and formation of hydrocarbon derived surface oxygenates, such as acetate, acrylate, formate, carbonate, and enolic species, by partial oxidation of the hydrocarbon, see, for example, ref 18. The adsorbed hydrocarbon oxygenate species can then react with nitrates to form N_2 or organo-nitro and -nitrite species (R-ONO and R-NO_2), which can lead to the formation of -NCO and/or -CN species. These species can further react with nitrates and O_2 to form N_2 or can be hydrolyzed by water to form NH_3 which, in turn, can react with NO_x to produce

dx.doi.org/10.1021/cs3001754 | ACS Catal. 2012, 2, 1615−1623

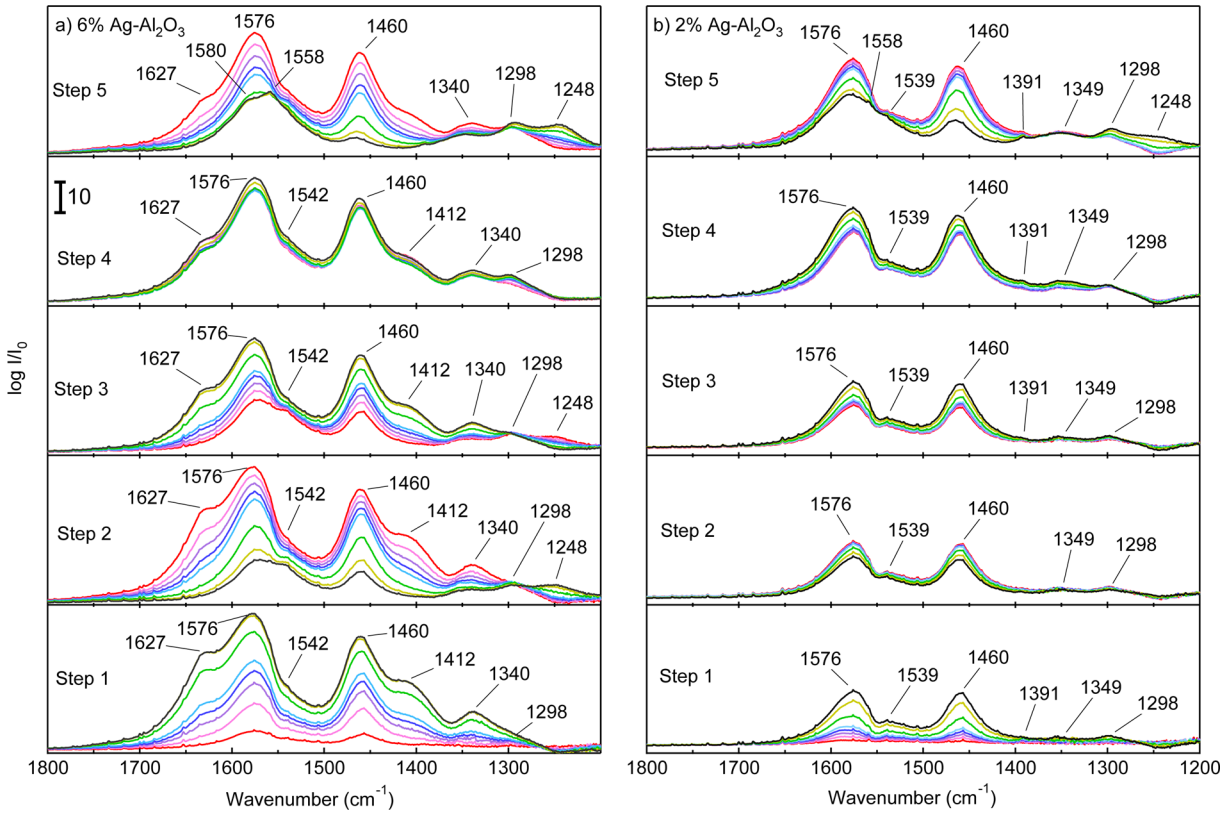

Figure 4. Evolution of surface species during step response experiments with C_2H_2 recorded in DRIFTS at 450 °C over Ag/Al_2O_3 catalyst with (a) 6 wt % and (b) 2 wt % nominal silver content, after 1 min (red), 2 min (pink), 3 min (purpule), 4 min (blue), 5 min (light blue), 10 min (green), 20 min (light green), and 30 min (black) gas exposure. Inlet gas composition: step 1: $C_2H_2 + O_2$; step 2: O_2; step 3: $C_2H_2 + O_2$; step 4: $C_2H_2 + NO + O_2$; step 5: $NO + O_2$. Contents: 600 ppm NO, 600 ppm C_2H_2, 10% O_2, Ar balanced.

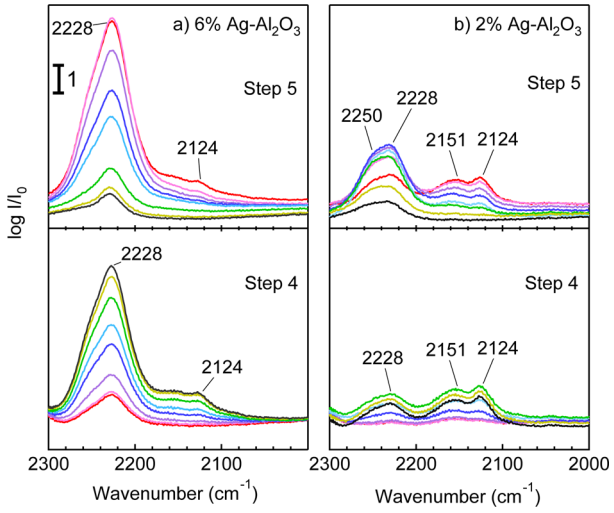

Figure 5. Evolution of surface species during step response experiments with C_2H_2 recorded in DRIFTS at 450 °C over Ag/Al_2O_3 catalyst with (a) 6 wt % and (b) 2 wt % nominal silver content, after 1 min (red), 2 min (pink), 3 min (purpule), 4 min (blue), 5 min (light blue), 10 min (green), 20 min (light green), and 30 min (black) gas exposure. Inlet gas composition: step 4: $C_2H_2 + NO + O_2$ and step 5: $NO + O_2$. Contents: 600 ppm NO, 600 ppm C_2H_2, 10% O_2, Ar balanced.

N_2.[21,48,58] The details in the reaction path, however, vary in different studies because of the difference in reactants, reaction conditions, and catalyst type and preparation.[7,21,52,55,58,59]

The nature of the surface species formed during hydrocarbon oxidation in this work seems to be more dependent on the type of hydrocarbon that is oxidized than on the silver loading of the catalyst. Oxidizing ethene in the presence of NO; acetate, formate, and carbonates as well as nitrate/nitrite are the most abundant surface species, and the evolution of the peaks related to these species nearly follows the same trend for both catalysts. When ethyne is oxidized in the presence of NO, on the other hand, some peaks evolve that are not observed for ethene. For instance, isocyanate and cyanide species are detected over the 2 and 6 wt % Ag catalysts for ethyne as reductant, whereas no isocyanate and/or cyanide species are observed when using ethene as reductant, except for a very weak band (2245 cm^{-1}), which may also be owing to NO^+ species.[54] The absence of a peak in DRIFTS experiments can be related to that the actual species is not formed during the specific reaction conditions or that the rates of formation and consumption of the specific species are equal. The latter seems to apply for the -NCO species observed here. Since -NCO surface species (2228 cm^{-1}) are formed and to some extent accumulated over the 6 wt % Ag sample in the presence of both C_2H_2 and NO (step 4) and then are consumed when the C_2H_2 supply is switched off, one can envisage that these species actually participate in the reaction. Over the 2 wt % Ag sample this is even more pronounced as both -NCO (2228 cm^{-1}) and -CN (2151, 2124 cm^{-1}) species are formed in the presence of C_2H_2 and NO. When the C_2H_2 supply is switched off, the -CN species diminish while the -NCO peak simultaneously increases, and after this the -NCO peak decreases again. This likely reflects a transformation of -CN to -NCO surface species followed by consumption of the

dx.doi.org/10.1021/cs3001754 | ACS Catal. 2012, 2, 1615−1623

-NCO species. The IR peaks presented in Figure 5 are very small compared to the IR peaks in Figures 3−4 (about one tenth in intensity), which emphasize the dynamics of these surface species, suggesting that they may be reaction intermediates rather than spectators. When C_2H_4 is oxidized (over both samples) in the presence of NO (step 4) a weak peak around 2245 cm^{-1} is formed. This peak increases slightly when the C_2H_4 supply is switched off (step 5). Considering this peak to be related to -NCO species, one would anticipate a consumption of -NCO species during step 5, in particular since water is present (formed) during both step 4 and step 5, and -NCO species are readily hydrolyzed with water forming amine species.[60] Since the 2245 cm^{-1} peak slightly increases instead we conclude that this peak likely is due to NO^+ species.[54] It is thus probable that the main reduction mechanism for ethene does not follow the reaction path via -NCO and -CN species, but instead proceeds through reduction of adsorbed nitrates by acetate and/or formate surface species. However, for both hydrocarbons, more surface species seem to be formed over the 6 wt % Ag catalyst as compared to the 2 wt % Ag catalyst. This can be related to the presence of more metallic silver particles in the 6 wt % Ag catalyst, which results in more facile activation of the hydrocarbons, and thus formation of more oxygenated hydrocarbon surface species.

An interesting feature in the DRIFTS experiments is the formation of formate. Arranging the experiments based on the formate-to-acetate ratio after 10 min (step 4), the following order is obtained: 2 wt % Ag -C_2H_4 > 6 wt % Ag -C_2H_4 > 2 wt % Ag -C_2H_2 > 6 wt % Ag -C_2H_2. As discussed previously, the 6 wt % Ag catalyst is more active for oxidation reactions than the 2 wt % Ag catalyst. Furthermore, C_2H_2 is a more easily activated hydrocarbon that is oxidized at lower temperatures compared to C_2H_4. Therefore, the formate-to-acetate ratio order (above) is inversely related to the ability whereby the catalyst can oxidize the hydrocarbon. This indicates that the probability of formate formation decreases as the oxidation ability of the hydrocarbon increases. This is further supported by the fact that formates can readily be formed from CO insertion into surface hydroxyls.[61] Hence, the formate formation can, at least partly, be related to the formation of CO, which is generally higher for the 2 wt % Ag sample. In other words, the tendency toward formation of formate surface species increases in less active reaction systems (i.e., less active hydrocarbon and less active catalyst for oxidation).

Shimizu et al.[50] have studied spectroscopically the SCR reaction over Ag−Al_2O_3, using *n*-octane as reducing agent, and reported bands at 1340, 1412, and 1627 cm^{-1}. These bands were assigned to carbonate species, which can cause poisoning according to the authors.[50] In our work these bands are observed only for ethyne over the 6 wt % Ag sample. The NO_x reduction is significantly lower for this sample as compared to the 2 wt % Ag sample (for ethyne). Hence, the lower NO_x reduction over the 6 wt % Ag catalyst may be related to the poisoning effect of carbonate species. On the other hand, the peaks at 1340, 1412, and 1627 cm^{-1} have also been attributed to enolic surface species,[58] using C_2H_5OH as reductant for NO_x over Ag/Al_2O_3. These results indicate that acetate species are predominant at high temperatures (500−600 °C), while enolic species become dominant at low temperatures (200−400 °C).[58] Further, the authors claim that the enolic surface species are more reactive in the formation of -NCO and -CN species compared to acetate. Our results imply that -NCO and -CN species are mainly formed when ethyne is used as reducing agent, and a higher amount is formed/accumulated over the 6 wt % compared to the 2 wt % Ag sample. However, because of overlapping of several of the IR bands, the origin for the formation of, for example, -NCO and -CN species is less certain. Enolic species may be one option since these peaks are observed in particular for the 6 wt % Ag sample with ethyne, and the highest amount of -NCO and -CN species is observed for this sample. Still the same peaks have also been assigned to carbonate surface species. Furthermore, in step 5, after 30 min, no traces of any enolic species can be observed, while both acetate and -NCO bands indicate that these species still remain on the catalyst surface. Therefore, another route for formation of -NCO species via surface acetates is also possible. Alternatively, the presence of -NCO species in step 5 can be an indication of accumulation of surface species from previous reaction steps.

4. CONCLUDING REMARKS

A systematic study of the influence of carbon−carbon bond order (C_2H_2, C_2H_4, and C_2H_6) and silver loading (2% and 6%) on the formation of partial oxidation products and lean NO_x reduction performance over silver-alumina catalysts is presented. Flow reactor experiments show that the highest activity for hydrocarbon oxidation and lean NO_x reduction is achieved when C_2H_2 is oxidized in the presence of NO. This is in accordance with the stronger interaction between ethyne and the metal surface, owing to the easily accessible π-electrons, a favorable molecular orientation, and higher sticking probability for C_2H_2 compared to the other C_2 hydrocarbons. For the studied hydrocarbons, the temperature window for NO_x reduction is broadened and shifted toward lower temperatures as the C−C bond order increases. Increasing the silver loading from 2 to 6 wt % is favorable for the oxidizing reactions, leading to activation of both hydrocarbons and NO_x at lower temperatures.

Generally in this study, the type of hydrocarbon seems to have a larger impact on the nature of the formed surface species and likely also on the surface processes than the silver loading. The 6 wt % Ag catalyst shows higher formation of surface species, owing to the presence of more metallic silver particles, than the 2 wt % Ag catalyst. For instance the formation of acetate, compared to formate, seems to be governed by a reactive hydrocarbon and a catalyst with more oxidizing sites, while the opposite is valid for formate formation. However, to receive good NO_x reduction performance both oxidizing and reducing sites are vital.

As demonstrated in this work the type of hydrocarbon determines the type of surface species formed during oxidation reactions. This needs to be considered when designing catalysts for emission control systems for different hydrocarbons, for example, alternative fuels. In particular for homogeneous fuels with short hydrocarbons, like methanol, ethanol, dimethyl ether, and methane, this work indicates that it may be possible to tailor the catalytic system at hand.

AUTHOR INFORMATION

Corresponding Author

*E-mail: hannahi@chalmers.se. Phone: +46 (0)31 7722959. Fax: +46 (0)31 160062.

Funding

This work has been performed at the Competence Centre for Catalysis, which is financially supported by Chalmers University

of Technology, the Swedish Energy Agency, and the member companies: AB Volvo, Volvo Car Corporation AB, Scania CV AB, Haldor Topsø A/S, and ECAPS AB. Financial support from Knut and Alice Wallenberg Foundation, Dnr KAW 2005.0055, and Area of Advance Transport are gratefully acknowledged.

Notes

The authors declare no competing financial interest.

REFERENCES

(1) Couves, J.; Atkins, M.; Hague, M.; Sakakini, B. H.; Waugh, K. C. *Catal. Lett.* **2005**, *99*, 45.
(2) Brosius, R.; Arve, K.; Groothaert, M. H.; Martens, J. A. *J. Catal.* **2005**, *231*, 344.
(3) Burch, R.; Breen, J.; Meunier, F. *Appl. Catal., B* **2002**, *39*, 283.
(4) Burch, R.; Breen, J. P.; Hill, C. J.; Krutzsch, B.; Konrad, B.; Jobson, E.; Cider, L.; Eränen, K.; Klingstedt, F.; Lindfors, L. E. *Topics Catal.* **2004**, *30*−*31*, 19.
(5) Shen, S. C.; Kawi, S. *Appl. Catal., B* **2003**, *45*, 63.
(6) Aoyama, N.; Yoshida, K.; Abe, A.; Miyadera, T. *Catal. Lett.* **1997**, *43*, 249.
(7) Kameoka, S.; Ukisu, Y.; Miyadera, T. *Phys. Chem. Chem. Phys.* **2000**, *2*, 367.
(8) Miyadera, T. *Appl. Catal., B* **1997**, *13*, 157.
(9) Miyadera, T. *Appl. Catal., B* **1993**, *2*, 199.
(10) Miyadera, T. *Appl. Catal., B* **1998**, *16*, 155.
(11) Shimizu, K.; Tsuzuki, M.; Kato, K.; Yokota, S.; Okumura, K.; Satsuma, A. *J. Phys. Chem. C* **2007**, *111*, 950.
(12) Kondratenko, E. V.; Kondratenko, V. A.; Richter, M.; Fricke, R. *J. Catal.* **2006**, *239*, 23.
(13) Kursawe, A.; Honicke, D. Comparison of Ag/Al- and Ag/alpha-Al2O3 Catalytic Surfaces for the Partial Oxidation of Ethene in Microchannel Reactors. In *Microreaction Technology*; Matlosz, M., Ehrfeld, W., Baselt, J. P., Eds.; Springer-Verlag: Berlin, Germany, 2001; pp 240−251.
(14) Arve, K.; Kannisto, H.; Ingelsten, H. H.; Eranen, K.; Skoglundh, M.; Murzin, D. Y. *Catal. Lett.* **2011**, *141*, 665.
(15) Kannisto, H.; Ingelsten, H.H.; Skoglundh, M. *J. Mol. Catal., A* **2009**, *302*, 86.
(16) Ingelsten, H.H.; Hellman, A.; Kannisto, H.; Gronbeck, H. *J. Mol. Catal., A* **2009**, *314*, 102.
(17) Shimizu, K.; Satsuma, A. *Phys. Chem. Chem. Phys.* **2006**, *8*, 2677.
(18) Burch, R. *Catal. Rev.* **2004**, *46*, 271.
(19) Kung, M. C.; Kung, H. H. *Topics Catal.* **2000**, *10*, 21.
(20) She, X.; Flytzani-Stephanopoulos, M. *J. Catal.* **2006**, *237*, 79.
(21) Shimizu, K.; Shibata, J.; Yoshida, H.; Satsuma, A.; Hattori, T. *Appl. Catal., B* **2001**, *30*, 151.
(22) Bogdanchikova, N.; Meunier, F.; Avalos-Borja, M.; Breen, J.; Pestryakov, A. *Appl. Catal., B* **2002**, *36*, 287.
(23) Meunier, F.; Breen, J.; Zuzaniuk, V.; Olsson, M.; Ross, J. *J. Catal.* **1999**, *187*, 493.
(24) Bethke, K.; Kung, H. *J. Catal.* **1997**, *172*, 93.
(25) Shi, C.; Cheng, M.; Qu, Z.; Bao, X. *Appl. Catal., B* **2004**, *51*, 171.
(26) Shibata, J.; Takada, Y.; Shichi, A.; Satokawa, S.; Satsuma, A.; Hattori, T. *J. Catal.* **2004**, *222*, 368.
(27) Brunauer, S.; Emmett, P. H.; Teller, E. *J. Am. Chem. Soc.* **1938**, *60*, 309.
(28) Barrett, E. P.; Joyner, L. G.; Halenda, P. P. *J. Am. Chem. Soc.* **1951**, *73*, 373.
(29) Dawody, J.; Skoglundh, M.; Wall, S.; Fridell, E. *J. Mol. Catal. A* **2005**, *225*, 259.
(30) Skoglundh, M.; Johansson, H.; Löwendahl, L.; Jansson, K.; Dahl, L.; Hirschauer, B. *Appl. Catal., B* **1996**, *7*, 299.
(31) Ingelsten, H. H.; Palmqvist, A.; Skoglundh, M. *J. Phys. Chem. B* **2006**, *110*, 18392.
(32) Matarrese, R.; Ingelsten, H. H.; Skoglundh, M. *J. Catal.* **2008**, *258*, 386.
(33) Djonev, B.; Tsyntsarski, B.; Klissurski, D.; Hadjiivanov, K. *J. Chem. Soc., Faraday Trans.* **1997**, *93*, 4055.
(34) Männikkö, M.; Skoglundh, M.; Ingelsten, H. H. *Appl. Catal., B* **2012**, *119*−*120*, 256.
(35) Breen, J. P.; Burch, R.; Hardacre, C.; Hill, C. J. *J. Phys. Chem. B* **2005**, *109*, 4805.
(36) Satokawa, S.; Shibata, J.; Shimizu, K.; Satsuma, A.; Hattori, T. *Appl. Catal., B* **2003**, *42*, 179.
(37) Blanksby, S. J.; Ellison, G. B. *Acc. Chem. Res.* **2003**, *36*, 255.
(38) Linic, S.; Jankowiak, J.; Barteau, M. A. *J. Catal.* **2004**, *226*, 245.
(39) Carlsson, P. A.; Mollner, S.; Arnby, K.; Skoglundh, M. *Chem. Eng. Sci.* **2004**, *59*, 4313.
(40) Carlsson, P. A.; Thormahlen, P.; Skoglundh, M.; Persson, H.; Fridell, E.; Jobson, E.; Andersson, B. *Topics Catal.* **2001**, *16*, 343.
(41) Ingelsten, H. H.; Skoglundh, M.; Fridell, E. *Appl. Catal., B* **2003**, *41*, 287.
(42) Siegbahn, P. *Theor. Chim. Acta* **1994**, *87*, 277.
(43) Solomons, T.W.G. *Organic Chemistry*, 5th ed.; John Wiley & Sons, Inc.: New York, 1992.
(44) Träskelin, P.; Saresoja, O.; Nordlund, K. *J. Nucl. Mater.* **2008**, *375*, 270.
(45) Kose, R.; Brown, W. A.; King, D. A. *Chem. Phys. Lett.* **1999**, *311*, 109.
(46) Davydov, A. A. *Infrared Spectroscopy of Adsorbed Species on the Surface of Transition Metal Oxides*; John Wiley & Sons: New York, 1990; p 39.
(47) Morterra, C.; Magnacca, G. *Catal. Today* **1996**, *27*, 497.
(48) Tamm, S.; Ingelsten, H. H.; Palmqvist, A. E. C. *J. Catal.* **2008**, *255*, 304.
(49) Meunier, F.; Zuzaniuk, V.; Breen, J.; Olsson, M.; Ross, J. *Catal. Today* **2000**, *59*, 287.
(50) Shimizu, K.; Satsuma, A.; Hattori, T. *Appl. Catal., B* **2000**, *25*, 239.
(51) Shimizu, K.; Kawabata, H.; Satsuma, A.; Hattori, T. *J. Phys. Chem. B* **1999**, *103*, 5240.
(52) Satsuma, A.; Shimizu, K. *Prog. Energy Combust. Sci.* **2003**, *29*, 71.
(53) He, H.; Zhang, C.; Yu, Y. *Catal. Today* **2004**, *90*, 191.
(54) Iglesias-Juez, A.; Hungria, A.; Martínez-Arias, A.; Fuerte, A.; Fernandez-Garcia, M.; Anderson, J.; Conesa, J.; Soria, J. *J. Catal.* **2003**, *217*, 310.
(55) Bion, N.; Saussey, J.; Haneda, M.; Daturi, M. *J. Catal.* **2003**, *217*, 47.
(56) Yu, Y.; Zhang, X.; He, H. *Appl. Catal., B* **2007**, *75*, 298.
(57) Hadjiivanov, K. I. *Catal. Rev.-Sci. Eng.* **2000**, *42*, 71.
(58) Yu, Y.; He, H.; Feng, Q.; Gao, H.; Yang, X. *Appl. Catal., B* **2004**, *49*, 159.
(59) Zuzaniuk, V.; Meunier, F. C.; Ross, J. R. H. *J. Catal.* **2001**, *202*, 340.
(60) Ingelsten, H. H.; Skoglundh, M. *Catal. Lett.* **2006**, *106*, 15.
(61) Liu, Z.; Li, X.; Ying, P.; Feng, Z.; Li, C. *J. Phys. Chem. C* **2007**, *111*, 823.